ENVIRONMENTAL SCIENCES Vol. 1, No. 1, 35~43
Bulletin of the Korean Environmental Sciences Society

A Simple Model for Dispersion in the Stable Boundary Layer

Sung-Dae Kang, Fujio Kimura,
Hwa-Woon Lee* and Yoo-Keun Kim*

Institute of Geoscience, University of Tsukuba, Ibaraki, Japan
**Department of Atmospheric Science, Pusan National University, Pusan, Korea*

(Manuscript Submitted 16 March, 1997)

Handling the emergency problems such as Chernobyl accident require real time prediction of pollutants dispersion. One-point real time sounding at pollutant source and simple model including turbulent-radiation process are very important to predict dispersion at real time.

The stability categories obtained by one-dimensional numerical model (including PBL dynamics and radiative process) are good agreement with observational data (Golder, 1972). Therefore, the meteorological parameters (thermal, moisture and momentum fluxes; sensible and latent heat; Monin-Obukhov length and bulk Richardson number; vertical diffusion coefficient and TKE; mixing height) calculated by this model will be useful to understand the structure of stable boundary layer and to handling the emergency problems such as dangerous gasses accident. Especially, this simple model has strong merit for practical dispersion models which require turbulence process but does not takes long time to real predictions.

According to the results of this model, the urban area has stronger vertical dispersion and weaker horizontal dispersion than rural area during daytime in summer season. The maximum stability class of urban area and rural area are "A" and "B" at 14 LST, respectively. After 20 LST, both urban and rural area have weak vertical dispersion, but they have strong horizontal dispersion. Generally, the urban area have larger radius of horizontal dispersion than rural area.

Considering the resolution and time consuming problems of three dimensional grid model, one-dimensional model with one-point real sounding have strong merit for practical dispersion model.

1. Introduction

The modelling of accidental scenarios in which radioactivity or other pollutants are released into the atmosphere is a common goal set out by both the environmentalist and by the nuclear community, which requires the help of flow modellers and air pollution meteorologists.

Following such an accidental release to the atmosphere, whether this involves radionuclides as in the case of the Chernobyl accident, or non-nuclear but hazardous and toxic materials an gasses, our ability to model and thereby to predict the specific atmospheric diffusion situation becomes uttermost importance for the subseqnent success or failure in the emergency handling of the off-site countermeasures.

Especially, to handling the emergency problems such as dangerous gasses accident, the understanding of characteristices of stability parameters in the stable surface boundary layer is very important, and practical diffusion models - which include turbulence process but does not takes long time to real predictions - are strongly

required.

There now exist a multitude of theoretical methods for making diffusion predictions for comparison with results of field and laboratory diffusion experiments. These include gradient transfer, spectral diffusivity second-order closure, large-eddy simulation, and random perturbation models (Briggs and Binkowski, 1985). However, these models generally require either detailed meteorological and turbulence measurements or many assumptions about these quantities, and may require considerable computational efforts.

For practical dispersion model, making simple correlations between the diffusion variables and key meteorological variables are required. Such correlations may be imperfect, but are still of great utility for practical diffusion models.

The most popular method for estimating dispersion in the stable boundary layer is based on the stability classification system proposed by Pasquill (1957) and then modified by Gifford (1961) - PG system. This PG system was developed to estimate vertical and lateral plume width from a continuous source at various distances. Therefore, the PG system has special meaning for considering turbulence as practical model.

In this study, one-dimensional atmosphere model (including PBL dynamics and radiative process) are used to investigate the characteristics of stability parameters in the strong stable surface boundary-layer. To estimate the qualities of one dimensional model results, comparison with observational data are carried out.

To estimate the spatial distribution of pollutants using plume model, the stability classes are determined from the output variables (short wave radiation, net radiation and surface wind speed) of one-dimensional model, and then dispersion measure are calculated from the formulas recommended by Briggs (1973).

2. Numerical model

The practical dispersion model require one-point observation data (wind speed at $10\,m$ height, short wave radiation and net radiation) at pollutants source. In this study, those one-point observational data are replaced by the output values of one-dimensional numerical model.

Assuming hydrostatic, incompressible and horizontal uniform conditions, the basic equations of PBL are :

$$\frac{\partial u}{\partial t} = f(v - v_g) + \frac{\partial}{\partial z} Km \frac{\partial u}{\partial z}, \qquad (2.1)$$

$$\frac{\partial v}{\partial t} = -f(u - u_g) + \frac{\partial}{\partial z} Km \frac{\partial v}{\partial z}, \qquad (2.2)$$

$$\frac{\partial \theta}{\partial t} = \frac{\partial}{\partial z} K_\theta \frac{\partial \theta}{\partial z} - \frac{1}{\rho C_p} \frac{\partial F_N}{\partial z}, \qquad (2.3)$$

$$\frac{\partial q}{\partial t} = \frac{\partial}{\partial z} K_q \frac{\partial q}{\partial z}, \qquad (2.4)$$

where, u, v, u_g, and v_g are horizontal and geostrophic wind components in x and y directions, respectively; θ is the potential temperature, and q is specific humidity. The second term of the right hand side of eq.(2.3) is the divergence of longwave radiation flux (Katayama scheme). Second order closure scheme (Mellor and Yamada, 1982) is used to close the model. Surface temperature is calculated from force restore method (Deardorff, 1978). A staggered grid scheme is used in the vertical direction. The top of the atmospheric model is $5\,km$ and bottom of soil model is $-1\,m$. The vertical mesh numbers of atmospheric model and soil model are 25 and 10 level with irregular mesh interval, respectively.

3. Numerical domain

Figure 1 show the schematic diagram of numerical domain. The geostrophic wind speed of

$5\,ms^{-1}$ is given at the level of $5\,km$, and very stable boundary layer is assumed; lapse rate is 6 $℃\,km^{-1}$. The stack (source of pollutants) having $100\,m$ height (see the caption "C" in this figure) is located in the stable surface boundary layer. In this figure, QS, QE, QH and QG indicate the amounts of shortwave radiation, sensible heat flux, latent heat flux and ground heat flux, respectively. The boundary conditions of top and bottom are close and open, respectively.

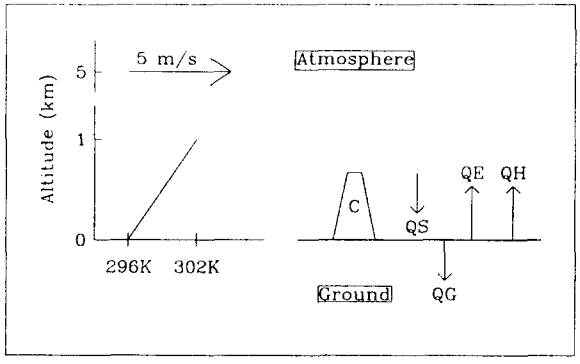

Fig. 1. The schematic diagram of numerical domain.

4. Numerical results

4.1. Characteristics of meteorological parameters in the stable boundary layer

The diurnal variations of ground temperature (o) and lower atmosphere temperature (*) are shown in Fig. 2. This figure show the time-variation of stability in the surface boundary layer. Before 9 LST, surface layer is stable, but after that, unstability become increase and then reach its maximum at 14 LST. The maximum value of ground temperature is 42 K at 14 LST, but the lower atmosphere temperature become its maximum values of 32 K at 17 LST. The surface layer become stable again after 19 LST.

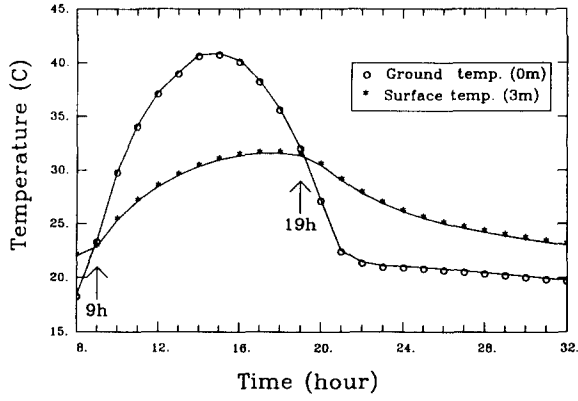

Fig. 2. The diurnal variations of ground temperature (o) and lower atmosphere temperature (*).

Figure 3 shows the diurnal variations of thermal, moisture and momentum fluxes in the surface layer. They have their maximum values of 0.13, 0.0014 and -0.07 at 15, 14 and 13 LST, respectively. The phase of thermal flux is similar to moisture flux, but momentum flux has negative phase. The thermal and moisture fluxes become positive after 9 LST and become negative after 20 LST. The momentum flux always maintain negative value.

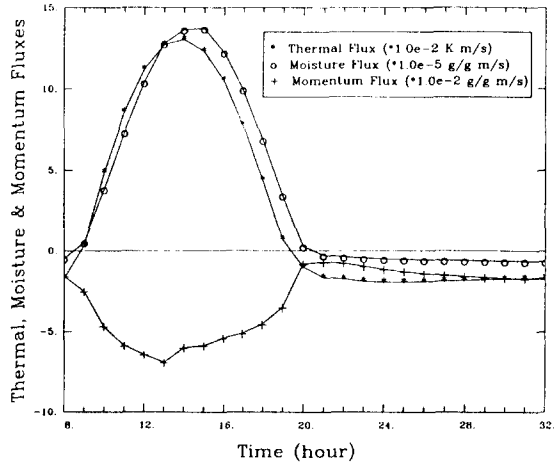

Fig. 3. The diurnal variations of thermal, moisture and momentum fluxes in the surface layer.

The tendencies of sensible and latent heat fluxes are shown in Fig. 4. In the case of strong stable atmosphere, the maximum difference between sensible and latent heat flux occur at 14 LST. The Bowen ratio at that time is about 0.35. In the early morning and evening, the Bowen ratio is almost equal to 1.

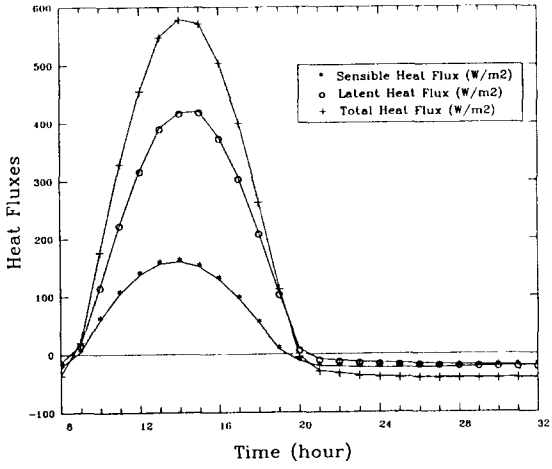

Fig. 4. The diurnal variations of sensible and latent heat fluxes on surface.

Figure 5 shows the diurnal variations of Monin-Obukhov length and bulk Richardson number in the stable surface layer. The maximum/minimum values of Monin-Obukhov length and bulk Richardson number are 0.0027/-0.0009 and 0.1/-0.1, respectively. They have the same phase and are proportion to the intensity of unstability; they become negative after 9 LST and have minimum value at 14 LST. While, they become positive after 19 LST and have maximum values at 21 LST.

In environmental meteorology, the mixing height is an important parameter because it defines the height to which pollutants, released at the ground, are vertically dispersed by convection or mechanical turbulence within a certain time scale of about an hour or less (Beyrich *et al.*, 1996). Radiosonde ascents still provide the most common database for mixing height estimation (e.g. Holzworth, 1972; Galinski *et al.*, 1995), which is also used in meteorological models (e.g. Olesen and Brown, 1992). Nevertheless, there is still no unique definition and no overall accepted method of mixing height determination. The equation of mixing height (z_i) used in this study is given below.

$$z_i = \sqrt{\frac{2}{\gamma}\int_0^t \overline{\theta w_0}\, dt}, \qquad (4.1)$$

where γ is atmospheric lapse rate.

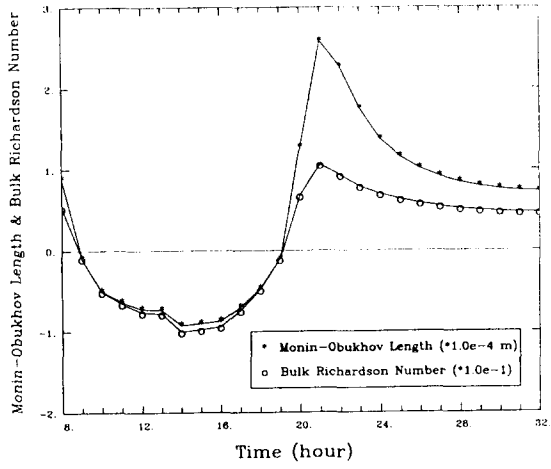

Fig. 5. The diurnal variations of Monin-Obukhov length and bulk Richardson number in the stable surface layer.

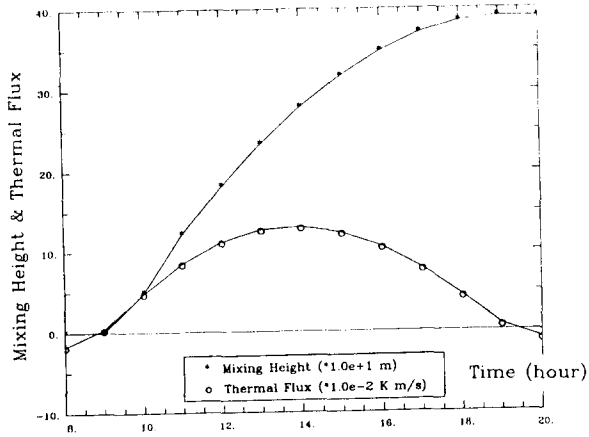

Fig. 6. The diurnal variations of both mixing height and thermal flux.

Figure 6 indicates the tendencies of both mixing height and thermal flux. The growth of mixing height depend on the amount of accumulated thermal flux, because the definition of mixing height is assumed only function of thermal flux(see eq. 4.1). The growth of mixing height begin after 9 LST and the maximum value is about 400 m at 19 LST.

Figure 7 shows the contours of vertical diffusion coefficient (a) and turbulent kinetic energy (b) on the time-altitude plane. The maximum values of them are 80 m^2s^{-1} and 100 m^2s^{-1}, respectively. The star dashed-line indicate the tendency of mixing height caused by thermal flux (see eq. 4.1). The maximum mixing height is related to the definition of mixing height. As shown in eq.(4.1), the definition of mixing height is lower than the altitude of maximum vertical diffusion of TKE. The reason may be only function of thermal flux and does not include the turbulence caused by wind shear in the atmosphere.

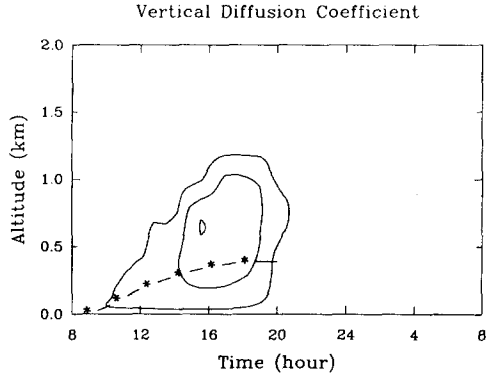

Fig. 7a.

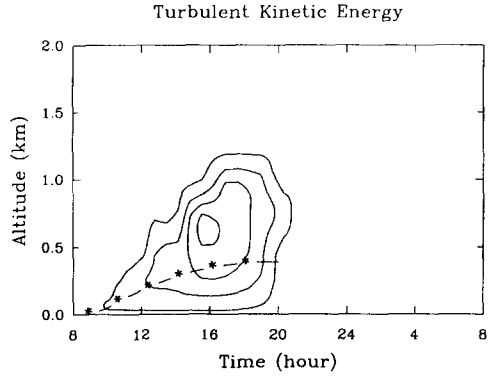

Fig. 7b.

Fig. 7. The contours of vertical diffusion coefficient (a) and turbulent kinetic energy (b) on the time-altitude plane.

4.2. Dispersion in the stable boundary layer

This section estimate the spatial distribution of pollutants at urban and rural area in the stable boundary layer.

The concentration (C) at x, y, z from a continuous source with an effective emission height, H, is given by the following equation.

$$C(x,y,z,H)=\frac{Q}{2\pi\sigma_y\sigma_z u}\exp\left[-\frac{1}{2}\left(\frac{y}{\sigma_y}\right)^2\right]$$
$$\left[\exp\left\{-\frac{1}{2}\left(\frac{z-H}{\sigma_z}\right)^2\right\}+\exp\left\{-\frac{1}{2}\left(\frac{z+H}{\sigma_z}\right)^2\right\}\right] \quad (4.2)$$

In the coordinate system considered here the origin is placed beneath the stack, with the x -axis extending horizontally in the direction of the mean wind. The y-axis is in the horizontal plane perpendicular to the x-axis, and the z -axis extends vertically.

In the above equation, the following assumptions are made: the plume spread has a Gaussian distribution in both the horizontal and vertical planes, with standard deviations of plume concentration distribution in the horizontal and vertical of σ_y and σ_z, respectively; the mean wind speed affecting the plume is u; the uniform emission rate of pollutants is Q; and total reflection of the plume takes place at the ground surface, i.e., there is no deposition or reaction at the surface. The most common units of C, Q and

Table 1. Pasquill's stability category

Wind speed m/s	Insolation $I \geq 50$	$50 > I \geq 25$	kW/m^2 $25 > I \geq 12.5$	$12.5 \geq I$	Net radiation $N > -1.8$	$-1.8 \geq N > -3.6$	$-3.6 \geq N$
< 2	A	A-B	B	D	D	G	G
2 ~ 3	A-B	B	C	D	D	E	F
3 ~ 4	B	B-C	C	D	D	D	E
4 ~ 6	C	C-D	D	D	D	D	D
6 <	C	D	D	D	D	E	D

Table 2a. Brigs's dispersion measure (urban area)

P-G stability	σ_y	σ_z
A-B	$0.32x(1+0.0004x)^{-1/2}$	$0.24x(1+0.0001x)^{-1/2}$
C	$0.22x(1+0.0004x)^{-1/2}$	$0.20x$
D	$0.16x(1+0.0004x)^{-1/2}$	$0.14x(1+0.0003x)^{-1/2}$
E-F	$0.11x(1+0.0004x)^{-1/2}$	$0.08x(1+0.0015x)^{-1}$

Table 2b. Brigs's dispersion measure (rural area)

P-G stability	σ_y	σ_z
A	$0.32x(1+0.0004x)^{-1/2}$	$0.20x$
B	$0.22x(1+0.0004x)^{-1/2}$	$0.16x(1+0.0004x)^{-1/2}$
C	$0.16x(1+0.0004x)^{-1/2}$	$0.22x(1+0.0004x)^{-1/2}$
D	$0.22x(1+0.0004x)^{-1/2}$	$0.16x(1+0.0004x)^{-1/2}$
E	$0.16x(1+0.0004x)^{-1/2}$	$0.14x(1+0.0003x)^{-1/2}$
F	$0.11x(1+0.0004x)^{-1/2}$	$0.08x(1+0.0015x)^{-1}$

u are gm^{-3}, gs^{-1} and ms^{-1}, respectively. The others (σ_x, σ_z, H, x, y, and z) have meter unit.

Stability categories (in six classes) are given in Table 1. Class "A" is the most unstable, class "F" the most stable class considered here. Its categories, which range from A to F, are each associated with curves for the dispersion measure σ_x and σ_z (see Table 2). The dispersion measures are estimated from the stability of the atmosphere, which is in turn estimated from the wind speed at a height of about 10 meters and, during the day, the incoming solar radiation or, during the night, the amount of net radiation.

Table 2 shows the analytical fits which derived by combining the PG curves with curves obtained from observation of elevated releases made at Brookhaven National Laboratory (Briggs, 1973). Table 2a and 2b are rural and urban area, respectively.

Figure 8 shows the comparison of stability categories between this model and Golder(1972). The curve fitting (solid line in this nomogram) of roughness length and inverse of Monin-Obukhov length for each stability categories are obtained from field experiments by Golder. The plotted small character indicate the stability class determined by one-dimensional model. This figure show that the stability categories determined from one-dimensional model are good agreement with observational data; especially, at A, B, and F classes.

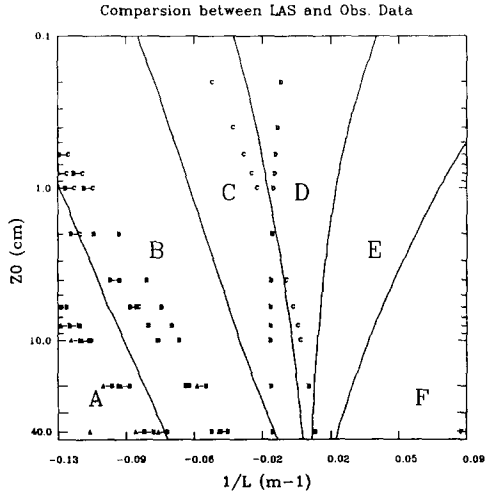

Fig. 8. The comparison of stability categories determined by this model with observational data (Golder, 1972).

The tendencies of stability categories for urban area are shown in Fig. 9. They are estimated by one-dimensional model under the conditions of roughness length (50 *cm*), amount of soil moisture (0.2) and stable atmosphere (lapse rate of 6 $℃ km^{-1}$). As the amount of solar insolation becomes increase in the morning, the absolute value of net radiation and the stability class also increase. The highest class of PG stability "A" is occur at 14 LST; the time when the amount of insolation and the absolute value of net radiation become maximum. The maximum values of insolation and absolute net radiation are 65.7 kWm^{-2} and 10.3 kWm^{-2}, respectively. The maximum and minimum values of surface wind velocities are 2.2 ms^{-2} and 1.4 ms^{-2}, respectively. After 20 LST, the stability class become "F". The amount of net radiation, instead of cloudness, is used to determine the stability categories in the night.

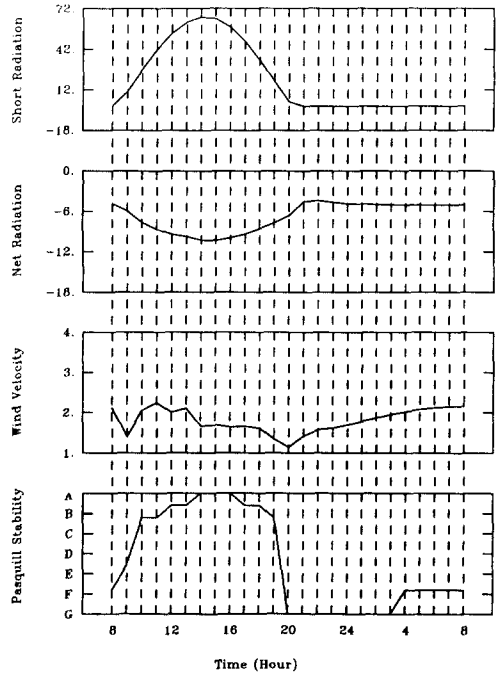

Fig. 9. The diurnal variations of stability categories for urban area.

Figure 10 shows the three-dimensional contour of pollutants for different time (a: 14 LST, b: 22 LST) at urban area. The pollutants are released at the top of stack having 100 *m* height. The stability classes of (a) and (b) are "A" and "F", respectively. Comparing (a) and (b), there are some relationship between stability class and the spatial dispersion intensity. If there are strong instability like case (a), the horizontal and vertical dispersions of pollutants in the lee of the stack are relatively weak and strong, respectively. However, if the boundary layer become strong in the lee of the stack.(stable like (b), the vertical dispersion become weak and horizontal dispersion become)

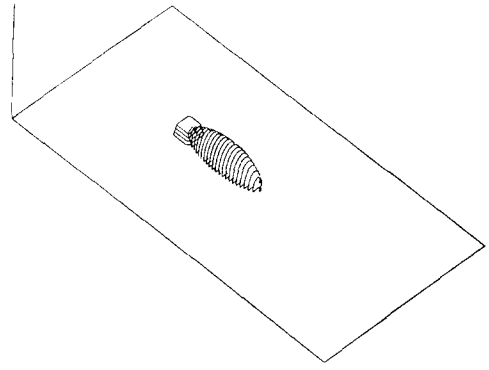

Fig. 10a.

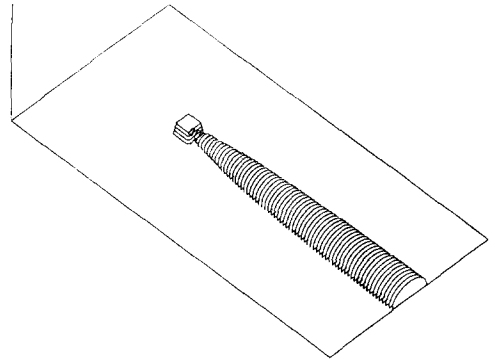

Fig. 10b.

Fig. 10. The three-dimensional contour of pollutants for different time (a: 14 LST, b: 22 LST) at urban area.

The tendencies of stability categories for rural area are shown in Fig. 11. Except that rural area having roughness length of 5 *cm*, the other conditions are the same as Fig. 9. The highest class of PG stability "B" is occur at 14 LST. The maximum values of insolation and absolute net radiation are 65.8 kWm^{-2} and 12.2 kWm^{-2}, respectively. The maximum and minimum values of surface wind velocities are 3.1 ms^{-2} and 1.8 ms^{-1}, respectively. After 20 LST, the stability class become "F". Comparing rural area with urban case (see Fig. 9 and Fig. 11), the amount of insolation and net radiation at rural area are about 0.1 kWm^{-2} and 1.9 kWm^{-2} higher than urban area, respectively

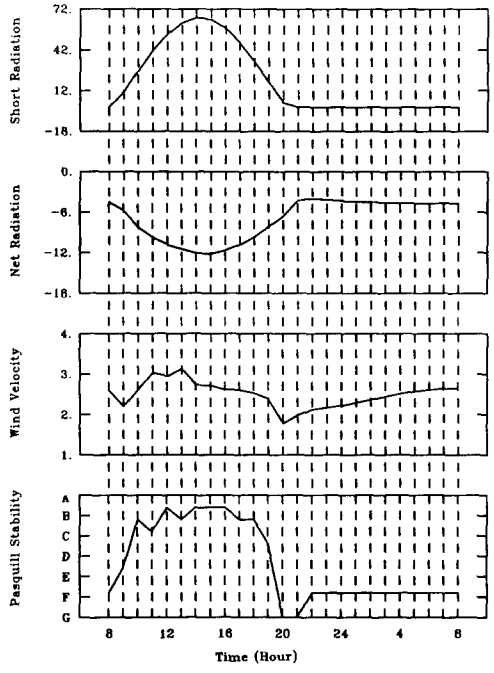

Fig. 11. The diurnal variations of stability categories for rural area.

Figure 12 shows the spatial distributions of pollutants for different time (a: 14 LST, b: 22 LST) at rural area. The pollutants are released at the top of stack having 100 *m* height like urban case. The stability classes of (a) is "B" and (b) is "F". At 14 LST, the horizontal dispersions of pollutants in the lee of the stack is weak and vertical dispersion is strong. However, the vertical dispersion become weak and horizontal dispersion strong after 22 LST.

Comparing urban area with rural area (See Fig. 10 and Fig. 12), the urban area has stronger vertical dispersion and weaker horizontal dispersion than rural area during daytime. The maximum stability classes of urban and rural area are "A" and "B" at 14 LST, respectively. After 20 LST, both urban and rural area have weak vertical dispersion, but they have strong horizontal dispersion.

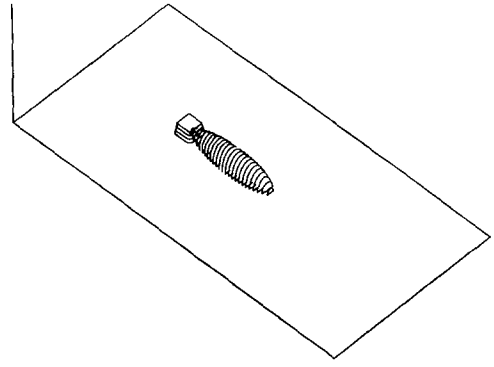

Fig. 12a.

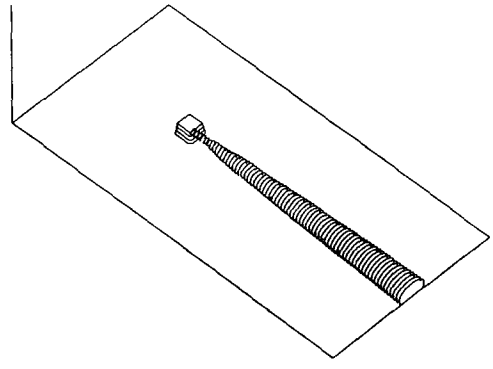

Fig. 12b.

Fig. 12. The three-dimensional contour of pollutants for different time (a: 14 LST, b: 22 LST) at rural area.

5. Conclusion

In this study, the stability categories estimated by one-dimensional numerical model are good agreement with the observational data (Golder, 1972). Therefore, the meteorological parameters (thermal, moisture and momentum fluxes; sensible and latent heat; Monin-Obukhov length and bulk Richardson number; vertical diffusion coefficient and TKE; mixing height) calculated by this model can be used to understand the structure of stable boundary layer.

The stability of the atmosphere is estimated from the wind speed at a height of about 10 meter and, during the day, the incoming solar radiation or, during the night, the amount of net radiation (see Table 1). The dispersion measures are estimated by the Brig's table for urban and rural cases (see Table 2), and then the spatial distributions of pollutants are estimated by plume model.

Comparing the dispersion of urban area with rural case (See Fig. 10 and Fig. 12), the urban area stronger vertical dispersion and weaker horizontal dispersion than rural area during daytime in summer season. The maximum stability class of urban area and rural area are "A" and "B" at 14 LST, respectively. After 20 LST, both urban and rural area have weak vertical dispersion, but they have strong horizontal dispersion. Generally, the urban area have larger radius of horizontal dispersion than rural area.

Considering the resolution and time consuming problems of three dimensional grid model, one-dimensional model with one-point real sounding have strong merit to handling the emergency problems as practical model.

Acknowledgements

The authors thank for two anonymous reviewers.

References

Beyrich, F., 1996, On the determinination of mixing height, *Preprints of the 4th workshop on Harmonisation within atmospheric dispersion modeling for regulatory purpose.*, pp.155-162.

Briggs, G. A., 1973, Diffusion estimation for small emissions, *1973 annual report, Environmental Res. Lab.*, report ATDL-106.

Binkowski, F. S., 1985, Research on diffusion in atmospheric boundary layers, a position paper on status and needs, *U. S. Environmental Protection Agency*, EPA/600/S3-85-072.

Deardorff, J. W., 1978, Efficient prediction of ground surface temperature and moisture, with inclusion of a layer of vegetation, *J. Geophys. Res.*, 83, 1889-1903.

Galinski, A. E., and D. J. Thomson, 1995, Comparison of three schemes for predicting surface sensible heat flux, *Bound. Lay. Meteor.*, 72, 345-370.

Golder, D., 1972, Relations among stability parameters in the surface layer, *Bound. Lay. Meteor.*, 3, 47-58.

Mellor, G. L., and Yamada, T., 1982, Development of a turbulence closure models for geophysical fluid problems, *Rev. Geophys. Space Phys.*, 20, 851-875.

Olesen, H. R., A. B. Jensen, and N. Brown, 1992, The OML meteorological preprocessor, *National Environmental Research Institute.*, MST LUFTA122.